# MIT Libraries | DSpace@MIT

# MIT Open Access Articles

## Prognosis of Component Degradation Under Uncertainty: A Method for Early Stage Design of a Complex Engineering System

# Massachusetts Institute of Technology

# ESDA2012-82420

# DRAFT: PROGNOSIS OF COMPONENT DEGRADATION UNDER UNCERTAINTY: A METHOD FOR EARLY STAGE DESIGN OF A COMPLEX ENGINEERING SYSTEM

**Bo Yang Yu, Tomonori Honda,* Gina M. Zak,
Alexander Mitsos, John Lienhard, Karan Mistry**
Department of Mechanical Engineering
Massachusetts Institute of Technology
Cambridge, MA 02139

**Syed Zubair, Mostafa H. Sharqawy, Mohamed Antar**
Mechanical Engineering Department
King Fahd University of Petroleum and Minerals
Dhahran 31261
Saudi Arabia

**Maria C. Yang**
Mechanical Engineering and Engineering Systems
Massachusetts Institute of Technology
Cambridge, MA 02139

## ABSTRACT

*This paper proposes a method that dynamically improves a statistical model of system degradation by incorporating uncertainty. The method is illustrated by a case example of fouling, or degradation, in a heat exchanger in a cogeneration desalination plant. The goal of the proposed method is to select the best model from several representative condenser fouling models including linear, falling rate, and asymptotic fouling, and to validate and improve model parameters over the duration of operation. Maximum likelihood estimation (MLE) was applied to obtain a stochastic distribution of condenser fouling. Akaike's Information Criterion (AIC) and the Bayesian Information Criterion (BIC) were then computed at time intervals to assess the accuracy of the MLE results. The degradation model was further evaluated by estimating future prognoses and then cross-validating with real world fouling data. The results show the accuracy of a prognosis can be improved substantially by continuously updating fouling model parameters. The proposed method is a step toward facilitating prognosis of engineering systems in the early design stages by improving the prediction of future component degradation.*

## Nomenclature

| | |
|---|---|
| $\Delta_j$ | difference in Information Criterion between model $f_j$ and minimum $IC$ |
| $\mathscr{L}$ | likelihood function |
| $\mu$ | mean |
| $\Phi$ | average log likelihood of samples collected between updates |
| $\sigma$ | standard deviation |
| $\tau$ | time constant in asymptotic fouling model |
| $\theta$ | model parameters |
| $\{f_1, f_2, ..., f_m\}$ | set of hypothetical models |
| $F_U$ | update frequency |
| $IC$ | Information Criterion |
| $k$ | number of free parameters in the model |
| $m$ | number of hypothetical models in a pool of possible models |
| $N$ | number of data points used in MLE |
| $N_f$ | samples per update |
| $N_i$ | initial number of samples |

---

*Address all correspondence to this author, tomonori@mit.edu.

1

| | |
|---|---|
| $R_f$ | fouling resistance |
| $R_{PC}$ | prognosis criterion |
| $t_d$ | initial fouling deposition time |
| $t_s$ | sample period |
| $U$ | overall heat transfer coefficient of a heat exchanger |
| $U_c$ | overall heat transfer coefficient at clean condition |
| $R_f{}^*$ | asymptotic fouling resistance |
| AICc | Akaike's information criterion |
| BIC | Bayesian information criterion |

## INTRODUCTION

Large-scale complex systems, such as industrial plants and space systems, can consist of any number of sub-systems and components. These components degrade over time, and inadequate maintenance of the components can result in high operational cost, increased environmental impact, as well as concerns about safety [1, 2].

Traditional maintenance scheduling commonly focus on both corrective (fix-as-fail) or preventive (regularly timed interval) strategies [1]. A corrective strategy does not schedule maintenance until failure has occurred, which can lead to long or inconvenient downtimes. A preventive strategy schedules maintenance according to the expected lifetime of a component, however, due to the uncertainty associated with component degradation, maintenance is often performed unnecessarily resulting in excessive cost. A more cost-effective maintenance strategy is to perform *health monitoring and prognosis* [3]. This strategy begins with the continuous monitoring of *degradation*, or the gradual reduction in performances of a subsystem or component over time. Health monitoring then makes predictions about future degradation based on past information, and provides dynamic scheduling decisions to maximize performance and reliability, while minimizing maintenance cost.

Interests in health monitoring and prognostics extend across a variety of engineering fields, from monitoring damage in mechanical structures [4], estimation of battery life [5], and power plant condition monitoring [1]. Several challenges are associated with the development of health monitoring systems. One is to quantify the amount of degradation using different sensor technologies, known as condition monitoring. Current research in this field has mostly been focused on failure-detection, isolation and identification using data-driven and/or model-based techniques [6, 7].

A second challenge is in *degradation modeling*, which is the characterization of the evolution of degradation signals by combining observations and physical understanding of the component [8]. A significant amount of research has focused on degradation models. Lu & Meeker [9] have studied numerical methods for fitting parametric models to degradation measurements and estimation of time-to-failure distribution. Zuo, Jiang & Yam [10] introduced three approaches for reliability modeling of continuous state devices, based on the random process model, the general path model, and the multiple linear regression model. Zhou, Serban & Gebraeel [11] presented a study on estimating degradation models with sparse or incomplete data. Wang & Coit [8] illustrated methods for dealing with uncertain failure thresholds in degradation modeling. There are also studies on the degradation models of a specific device. Saha & Goebel [5] describe a technology for using a particle filtering framework combined with an empirical model for battery life prediction. Zubair et al. [12, 13] have studied statistical models to describe heat transfer component degradation. Prasad et al. reported an algorithm developed by GE capable of predicting degradation in heat exchangers [14].

However, current studies on degradation modeling and time-to-failure estimations do not focus on real-time model estimation, or dynamic assessment of prediction accuracy. Thus, this study focuses on the development of a prognosis scheme that combines degradation monitoring and future performance prediction. The proposed scheme is composed of two parts: dynamic predictions based on continuously collected operational data, and continuous assessment of the accuracy of the prediction. A case example of degradation in heat exchangers in a cogeneration desalination plant is used for illustration.

## METHOD

The step by step illustration of the prognosis process is shown in the flow chart in Fig. 1. A pool of $m$ possible degradation models $\{f_1, f_2, ..., f_m\}$ should first be assembled and the most appropriate model can be selected based on the collected degradation data. The monitoring program will record operation data from the system and compute the degradation at some sampling period $t_s$. After some initial number of samples $N_i$ has been obtained, model parameters for each model in the pool can be inferred based on the data ($N_i$ have to be large enough for the inference algorithm to avoid over fitting). Then the models are compared to each other and one that best describes the current degradation process is determined. Using the best model, maintenance prognosis can be made. If maintenance is not required and operation continues, more operation data is collected and used in the next prognosis period. The prognoses frequency is determined by the sampling time $t_s$ as well as the number of samples collected between each prognosis $N_f$, which is typically equal to or less than $N_i$. The values of $N_i$, $N_f$, and $t_s$ will affect prognosis process, and will be discussed in detail in the next section. For typical operation, prognoses will occur at

$$t = \{t_1, t_2, t_3, ...\} = \{N_i t_s, (N_i + N_f)t_s, (N_i + 2N_f)t_s, ...\} \quad (1)$$

and the update frequency $F_U$, which indicate how often prognoses is performed, is:

$$F_U = \left(N_f t_s\right)^{-1} \tag{2}$$

Statistical inference is used in this study to estimate the model parameters by fitting to the measured degradation data. Maximum likelihood estimation (MLE) is proposed for fitting because of its ability to fit any type of probability distribution, whereas traditional least-square error curve fitting methods are limited to normally distributed variations. The maximum likelihood estimation is defined as:

$$\theta_{mle} = \arg\max\{\log(\mathscr{L}_i)\} \tag{3}$$

where $\theta_{mle}$ is the set of model parameters that maximizes the log likelihood function $\log(\mathscr{L}_i)$ of model $f_i$ (argument of the maximum). The likelihood function $\mathscr{L}$ of model $f$ given the set of data $\bar{x} = \{x_1, x_2, ..., x_N\}$ is defined as:

$$\mathscr{L}(\theta|\bar{x}) = \prod_{j=1}^{N} f(x_j|\theta) \tag{4}$$

where $f(x_j|\theta)$ is the probability distribution function of model $f$ with parameters $\theta$.

An information criterion can be used to select the most accurate model from the pool. Akaike's information criterion (AIC) and the Bayesian information criterion (BIC) are commonly used. AIC is an estimated measurement of the information loss when a model is used to describe reality, and can be calculated by minimizing Kullback-Leibler information entropy using the formula:

$$\text{AICc} = -2\log(\mathscr{L}) + 2k\left(\frac{N}{N-k-1}\right) \tag{5}$$

The lower case c represents the corrected AIC, which takes into account the number of available data. $\mathscr{L}$ is the log likelihood obtained from MLE, $k$ is the number of free parameters in the model, and $N$ is the number of data points used in the estimation. A low AICc number indicates less information loss and thus is more desirable. The AICc formula suggests that information loss is closely related to the likelihood value, and inversely related to the number of parameters in the model to penalize over fitting.

BIC is an estimation of the Bayesian posterior probability associated with a model. It has a very similar form to AICc with a more stringent penalty for over fitting.

$$\text{BIC} = -2\log(\mathscr{L}) + k\log(N) \tag{6}$$

Comparatively, AIC and BIC take very different approaches to model selection: AIC selects the model that most adequately describes reality, and BIC selects the model that most likely represents reality. For a large sample size, AIC favors complex models with high number of free parameters and tend to result in over fitting, while for a small sample size BIC will favor complex models. The model with the smallest information criterion is the best among the pool of models. In general, if AIC and BIC are in agreement, then the most optimal model can be selected. The probabilities of model $f_j$ being the best model can be computed based on the information criterion using the formula:

$$p(f_j|\{f_1, f_2, ..., f_m\}) = \frac{\exp\left(-\frac{1}{2}\Delta_j\right)}{\sum\limits_{r=1}^{m} \exp\left(-\frac{1}{2}\Delta_r\right)} \tag{7}$$

where $\Delta_j$ is the Information Criterion (IC) difference between model $f_j$ and the minimum IC:

$$\Delta_j = IC(f_j) - IC_{min} \tag{8}$$

As more data become available, new model parameters can be estimated using more data samples, and should converge to the true model parameters. Thus a second criterion is proposed to test for the convergence of model parameters. Sample points from the future can be used to perform cross validation with the model prognoses by computing the likelihood of the model given these sample points. In reality, this can be done using data collected in the next monitoring period $t = t_{i+1}$ then cross-validated with the model estimated in the current monitoring period $t = t_i$:

$$\Phi(t_i) = \frac{1}{N_f} \log\left(\mathscr{L}\big(\theta(t_i)|\bar{x}(t_{i+1})\big)\right) \tag{9}$$

where $\Phi$ is the average log likelihood value of samples $\bar{x}$ collected between time period $t_i$ and $t_{i+1}$ given parameters $\theta$ estimated at time $t_i$. As the model parameters are refined with more sample points, the $\Phi$ value would level out to a certain value, as the model parameters converge to an optimal value. If the model is an inadequate representation of reality, the model parameters do not converge, and thus $\Phi$ value will fail to converge. A proposed convergence criterion that we call a *prognosis criterion* ($R_{PC}$) is defined as:

$$R_{PC}(t_i) = \Phi(t_i) - \Phi(t_{i-1}) \tag{10}$$

which will approach zero as model parameter values converge.

Different scenarios can occur with the prognosis criterion. For example, there may be a sudden divergence trend in the prognosis criterion if the operating conditions changed suddenly. The
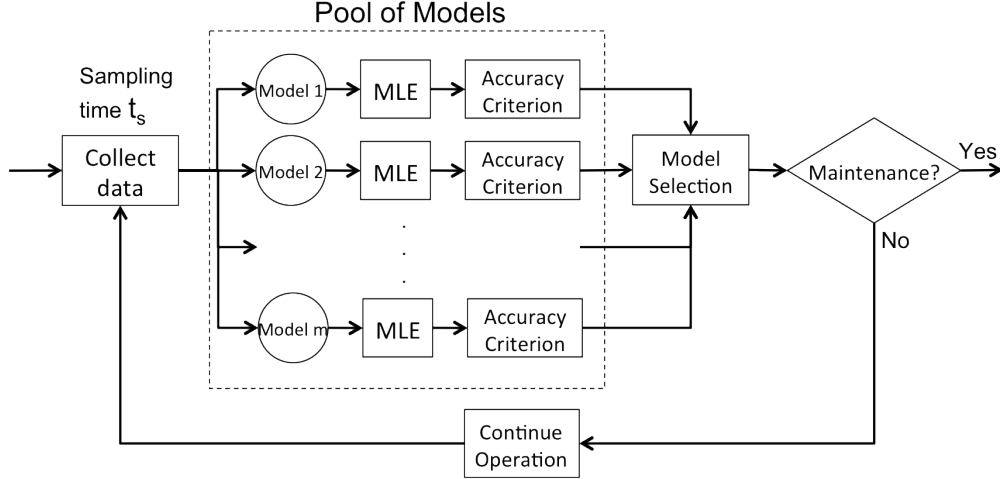
**FIGURE 1**. FLOWCHART OF PROGNOSIS STEPS

prognosis criterion for a bad model could also converge if the bad model predicts uncertainty very generously. In the next section different scenarios will be examined to induce the benefits of the prognosis criterion.

To summarize the prognosis method:

1. Assemble pool of hypothetical degradation models
2. Collect degradation data ($N_i$ samples initially, $N_f$ samples each time after)
3. Perform MLE model fitting using all samples collected
4. Compute model probabilities using AIC and BIC
5. If AIC and BIC results agree, select the model and compute $R_{PC}$, otherwise go back to step 2 and repeat
6. (Future work) Combine the selected model and $R_{PC}$ to produce a prognosis, and make scheduling decisions.

## CASE STUDY

This case example is of a cogeneration desalination plant for treating seawater. Such plants consist of boilers, heat exchangers, and other components. This example focuses on a heat exchanger whose degradation mode is fouling and scaling. The accumulation of unwanted particles on the heat transfer surfaces of heat exchangers are referred to as fouling (typically biological buildup) and scaling (typical hard salts, we will use the word "fouling" in this paper when referring to both fouling and scaling). This layer of deposit increases the thermal resistance of a heat exchanger and degrades its performance [15]. No technology currently exists to completely eliminate fouling, and thus periodic cleaning of a heat exchanger is required [16]. The ability to accurately predict a fouling trend and schedule optimal maintenance is important [12].

The amount of fouling in a heat exchanger is characterized by its fouling resistance $R_f$ with units (m$^2$K/W) [17]:

$$R_f = \frac{1}{U} - \frac{1}{U_c} \qquad (11)$$

where $U$ is the overall heat transfer coefficient of the heat exchanger, usually calculated from hot and cold fluids type, flow rates, pipe material and dimensions. $U_c$ is the overall heat transfer coefficient of the heat exchanger with clean surfaces. Although heat exchanger fouling is a complex stochastic process that depends on a variety of conditions, such as water quality, flow rate, temperature, and geometry, relatively simple statistical models can be used to approximate the fouling resistance-time relationship [12].

Typical heat exchanger fouling resistance vs. time curves observed in industry are shown in Fig. 2. The mathematical models of these curves were described by Zubair et al. [12] and are represented as:

$$\text{Linear rate (curve a): } R_f(t) = \mathbf{B}(t - t_d) \qquad (12)$$

$$\text{Falling rate (curve b): } R_f(t) = \mathbf{B}\log\left((t - t_d)/\tau + 1\right) \qquad (13)$$

$$\text{Asymptotic (curve c): } R_f(t) = \mathbf{R_f^*}\left(1 - e^{-(t - t_d)/\tau}\right) \qquad (14)$$

The initial deposition time $t_d$ shown in Fig. 2 is a period at the initial stage when the fouling deposition has not started to develop, which is a phenomenon occasionally observed in reality [17]. Curve d) in Fig. 2 is a typical representation of fouling in power plant condensers and cooling towers. The sawtooth shape is a result of periodic changes in operating conditions, for example seasonal water temperature change [17–19]. The variation of
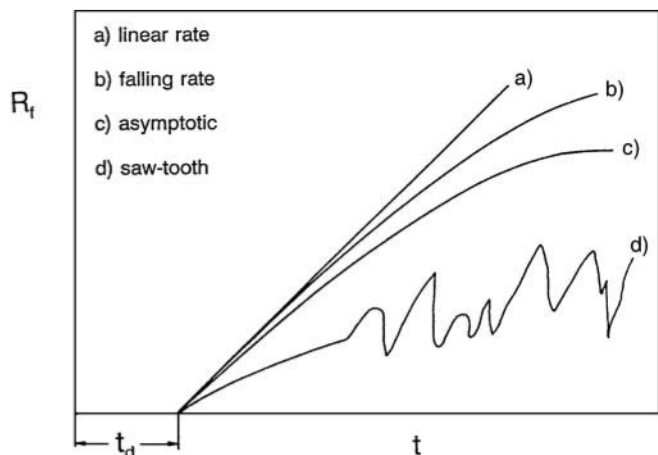
**FIGURE 2**.  TYPICAL FOULING TREND CURVES OVER TIME [15]

fouling resistance over time can be expressed as a probability distribution. Sheikh et al. [13] have suggested that the variables in the fouling models (**B** and $\mathbf{R_f^*}$) can be considered as normally distributed random variables with mean $\mu$ and standard deviation $\sigma$.

A number of semi-empirical formulae have been developed to estimate the parameters of a fouling model in a given application, but the general applicability of these formulae is limited because the various constraints or coefficients are plant dependent and difficult to measure [19, 20]. However, statistical inference methods can be used to estimate the model parameters based on data obtained from real time monitoring of the fouling process [14].

## ANALYSIS
### Artificial Fouling Simulation

Monte-Carlo simulations were first performed to test the proposed technique, to verify the model selection using AIC and BIC, as well as the effects of the operating parameters. Artificial fouling resistance data were simulated using the asymptotic model described in Eqn. 14, and shown here in non-dimensionalized form:

$$\frac{R_f}{R_f^*} = \mathcal{N}\left(1,\left(\frac{\sigma}{R_f^*}\right)^2\right)\left(1 - e^{-\frac{t}{\tau}}\right) \tag{15}$$

with $\frac{\sigma}{R_f^*}$ equal to 0.06 and $\tau$ equal to 1. These values represent a general asymptotic fouling process with uncertainty discussed in literature [19].

Two possible fouling models are assembled in the pool, one is identical to the underlying model (the asymptotic model), and a falling-rate model is chosen for comparison purposes because it has a similar shape to the asymptotic model:

Asymptotic model: $R_f(t) = \mathcal{N}(a_2, b_2) \cdot \left(1 - e^{c_2 t}\right)$     (16)

Falling-rate model: $R_f(t) = \mathcal{N}(a_1, b_1)\log(c_1 t + 1)$     (17)

A MATLAB$^{\circledR}$ (version 7.12) script was used to perform the simulation by generating random fouling resistances from the underlying model (Eqn. 15) at a user defined sampling time $t_s$ in non-dimensional time units, and compute prognosis at an update frequency $F_U$ with number of samples per update $N_f = (F_U \cdot t_s)^{-1}$.

**Model Fitting and Selection**   Figure 3 shows the Maximum Likelihood Estimation model fitting results using simulated data at three different times for one set of simulations, with parameters $N_i = N_f = 5$, $F_U = 4$. The MLE results are compared with the true underlying model used to generate the fouling data. After several updates it is observed that the asymptotic model has converged closely to the true model, while initially both models are quite different from reality, due to the small sample size.

The probabilities of each model computed at each update period are shown in Fig. 4. The model probability of the asymptotic model starts at around 0.5 and converges to 1 after some time (falling-rate probability is one minus asymptotic probability). The probability calculated using AIC and BIC are identical for these two models, because both models have the same number of free parameters.

Figure 5 shows the prognosis criterion $R_{PC}$ for this simulation. Both models show some oscillation in the result. The asymptotic model converges to zero and stays close to zero, while the falling-rate model has high oscillation and does not exhibit any convergence.
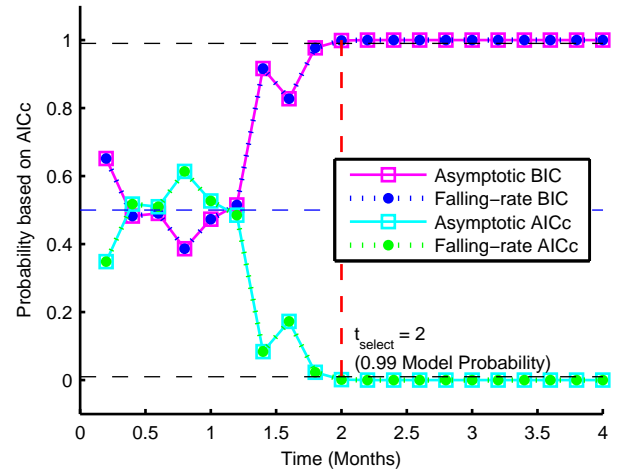
**Model Selection Criteria**   Next we would like to study how the operating parameters, including update frequency $F_U$ and number of samples per update $N_f$, as well as the uncertainty in the model ($\frac{\sigma}{R_f^*}$ term in Eqn. (15)), affect the model selection criteria mentioned above. Simulations were performed with varying values of $F_U$, $N_f$, and model uncertainty one at a time. 100 rounds of simulation were performed at each set of operating parameters.

To concisely illustrate the result, two critical times were defined to represent the rate of convergence for both the model probability and the prognosis criterion: 1) the model selection time $t_{select}$, which is the time when the Asymptotic model probability rises above 0.99. This critical time indicates our confidence
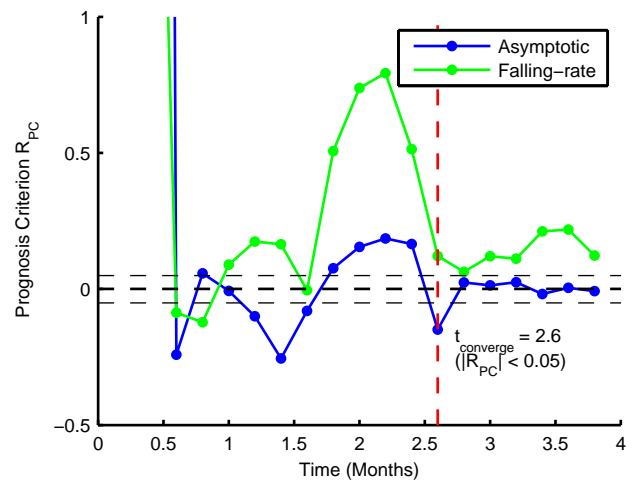
5
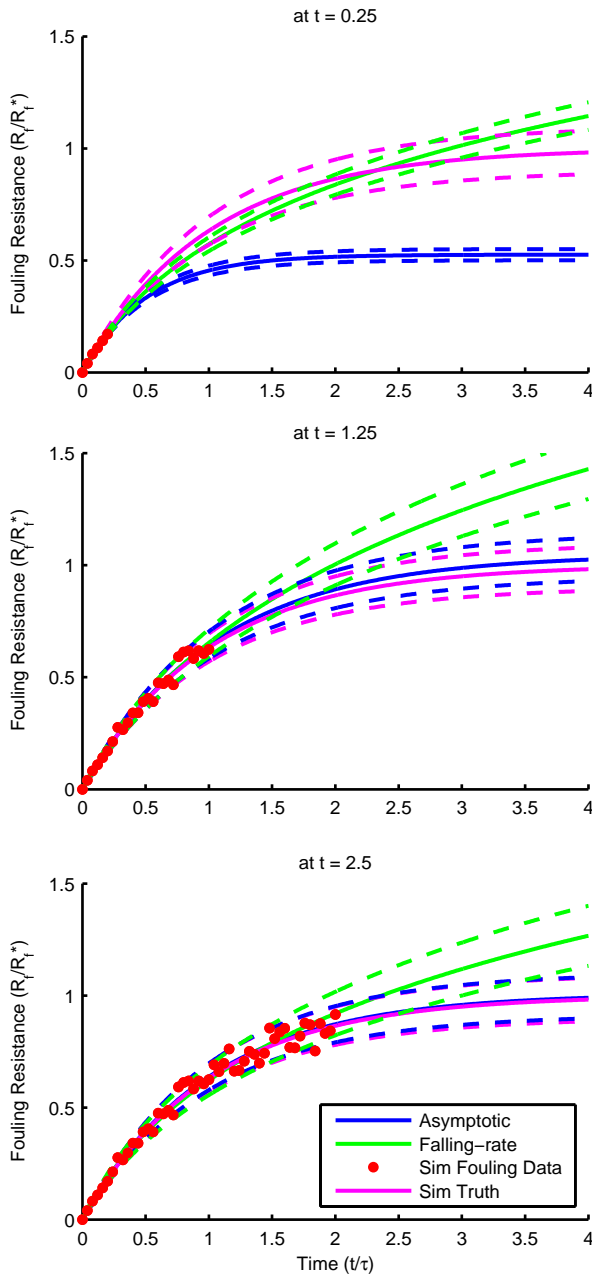
**FIGURE 3**. MLE RESULTS OF SIMULATED DATA THREE DIFFERENT TIMES. Dashed lines show the 5-95 percentile uncertainty region. Simulation performed with $N_i = N_f = 5$, $F_U = 4$



**FIGURE 4**. PROBABILITY OF MODELS AT EACH UPDATE. Simulation performed with $N_i = N_f = 5$, $F_U = 4$



**FIGURE 5**. PROGNOSIS CRITERIA AT EACH UPDATE. Simulation performed with $N_i = N_f = 5$, $F_U = 4$

in the model we have. 2) the prognosis convergence time $t_{converge}$, which is the time when the $R_{PC}$ of the Asymptotic model has fallen and remained between $\pm 0.05$. This critical time indicates the estimated model parameters have converged to their optimal

values (if optimal values exist). For both critical times a low value is desirable, suggesting higher confidence in model selection and prediction. The results of the simulations are presented in Fig. 6,7,8 in the form of critical times vs operating parameters.

As expected, higher updated frequency and higher number of samples per update decreases with both the model selection time $t_{select}$ and the prognosis convergence time $t_{converge}$, indicating more accurate prognosis results. However, the rates of decay for $t_{select}$ and $t_{converge}$ are different, resulting in diminishing re-
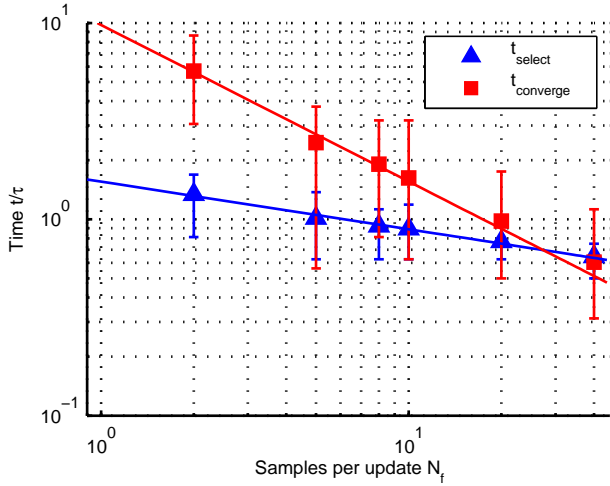
**FIGURE 6**. DECISION TIMES VS NUMBER OF SAMPLES PER UPDATE, $F_U = 8$. Plots showing average and 5-95 percentile region of 100 simulations, and least square fitting of power law curves
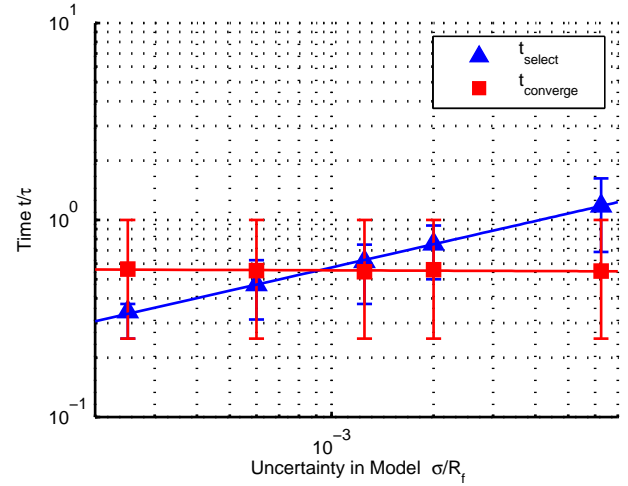


**FIGURE 8**. DECISION TIME VS UNCERTAINTY, $F_U = 8, N_f = 50$. Plots showing average and 5-95 percentile region of 100 simulations, and least square fitting of power law curves
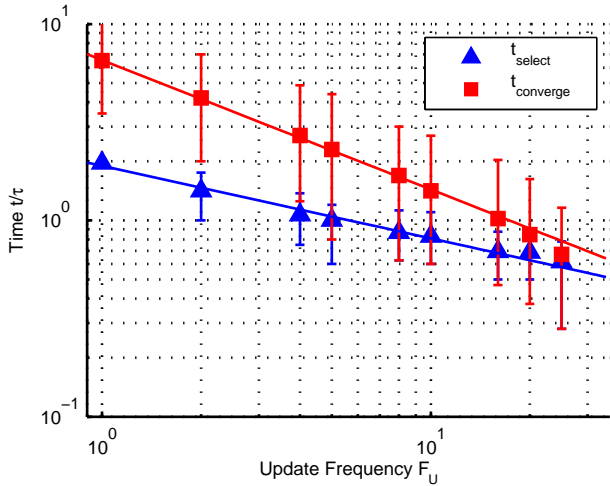


**FIGURE 7**. DECISION TIME VS UPDATE FREQUENCY, $N_f = 10$. Plots showing average and 5-95 percentile region of 100 simulations, and least square fitting of power law curves

The above analysis shows the ideal operating situation, where one hypothetical model matches the data very well, and thus both the model probability and the prognosis criterion indicate the same result. Next, two non-ideal scenarios are simulated. First is when no good model is available in the pool, and second when the model probability and the prognosis criterion show contradicting results. Studying these scenarios will help induce how the different criteria can be used for making prognosis.
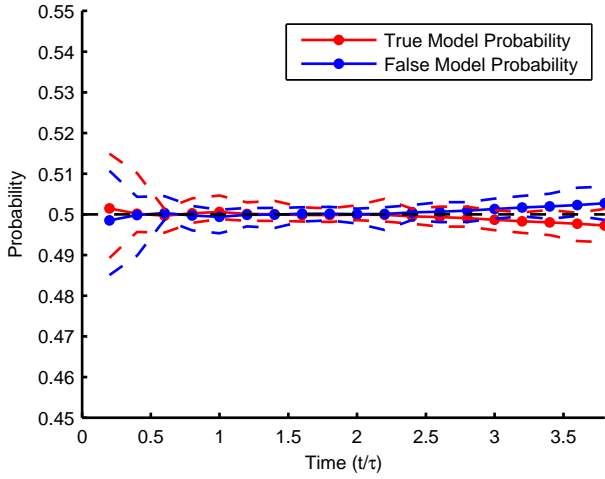
**Scenario when pool contains only poor models**  It is possible to have a scenario where all hypothetical models in the pool are poor representations of the reality. This scenario is simulated by generating artificial fouling resistance using a linear model shown below:

$$\frac{R_f}{R_f^*} = \mathcal{N}(0, 0.06)t \qquad (18)$$

and performing model fitting with the model pool consisting of an asymptotic model and a falling-rate model (Eqn. (16) and (17)) used in the previous sub-section. The operating parameters involved are $N_i = N_f = 5$, $F_U = 5$. These two models are very similar, both have the same number of free parameters, and both have an initial linear slope. The model probabilities are shown in Fig. 9.

The model probabilities show that both models are equally good at representing the data as the probability fluctuates slightly around 0.5. This scenario shows that when there is no good

turns at very high sampling and update frequency. The model uncertainty seems to affect only the model selection time, which suggests that if the form of the uncertainty is correctly modeled, then the relative accuracy of the prognosis is not affected by the variance of the uncertainty. The error bars on the convergence time are generally much wider compared to the selection time, suggesting that large variations are usually observed in the prognosis criterion. Thus time averaged values of $R_{PC}$ would be a better measurement than individual values.

**FIGURE 9**. AVERAGE MODEL PROBABILITY COMPUTED FROM AICC. Poor model pool scenario, average of 100 rounds of simulation. Dashed lines show 5-95 percentile region



**FIGURE 10**. AVERAGE MODEL PROBABILITY COMPUTED FROM AICC. Contradicting criteria scenario: average of 100 rounds of simulation. Dashed lines show 5-95 percentile region

model within the pool, this could lead to several models having the same probability. Conversely, if the model probability criterion does not indicate the selection of a single model with close to 100% probability even when many data points become available, it is likely that a better model is needed.

**Scenario with contradicting criteria** If a model significantly overestimates the uncertainty distribution of the degradation process, then the prognosis criterion may show a converging trend even if the model is inaccurate. A scenario similar to this is set up by generating artificial fouling resistance using Eqn. (19) below:

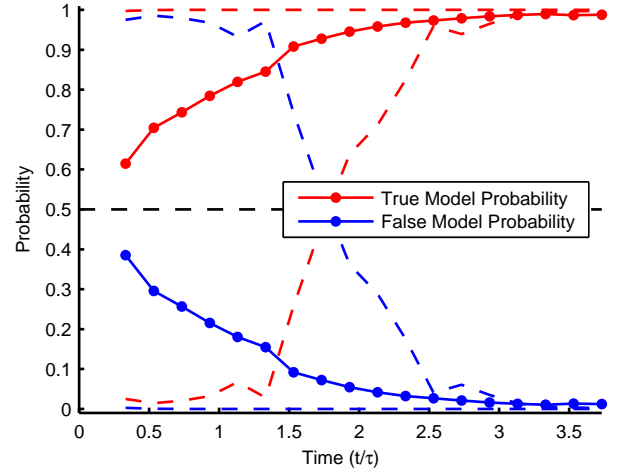$$\frac{R_f}{R_f{}^*} = (1 - e^{-t}) + \mathcal{N}(0, 0.06) \qquad (19)$$

and the model pool:

$$\text{True model: } R_f(t) = a_1 \left(1 - e^{c_1 t}\right) + \mathcal{N}(0, b_1) \qquad (20)$$
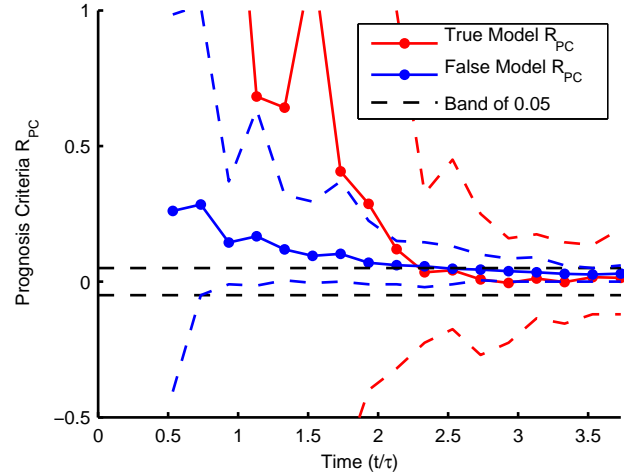
$$\text{False model: } R_f(t) = \mathcal{N}(a_2, b_2) \cdot \left(1 - e^{c_2 t}\right) \qquad (21)$$

with $N_i = 5$, $N_f = 3$, $F_U = 5$. The only difference between the models is that the false model assumes model uncertainty increases with time. The model probability and prognosis criterion of one hundred rounds of simulation is shown in Fig. 10 and Fig. 11.

The model probability points out the true model very early on, however the the ratios of prognosis criterion $R_{PC}$ show sig-
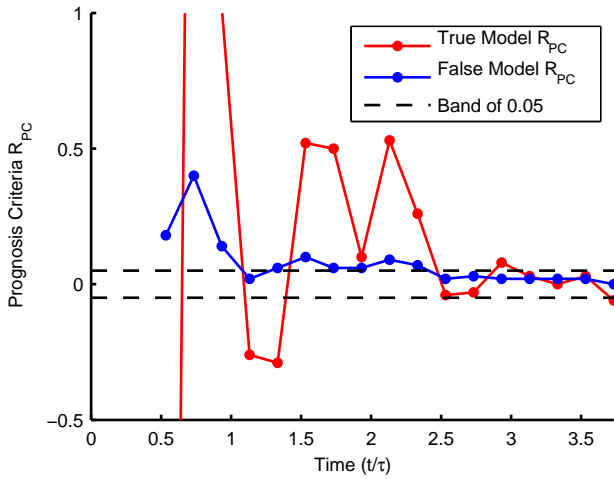


**FIGURE 11**. AVERAGE PROGNOSIS CRITERION. Contradicting criteria scenario: average of 100 rounds of simulation. Dashed lines show 5-95 percentile region

nificant oscillation for the true model (one instance of the simulation shown in Fig. 12), while showing a very smooth and converging trend for the false model. The average value of $R_{PC}$ of the true model also stays further away from zero compared to the false model from zero. The high oscillation indicates that model parameters can change significantly at each update and that predicting into the future using this model is unreliable until more data is gathered and $R_{PC}$ converged close to zero.

The analyses done on the model selection method and the

8

**FIGURE 12.** PROGNOSIS CRITERION. Contradicting criteria scenario: one instance of simulation
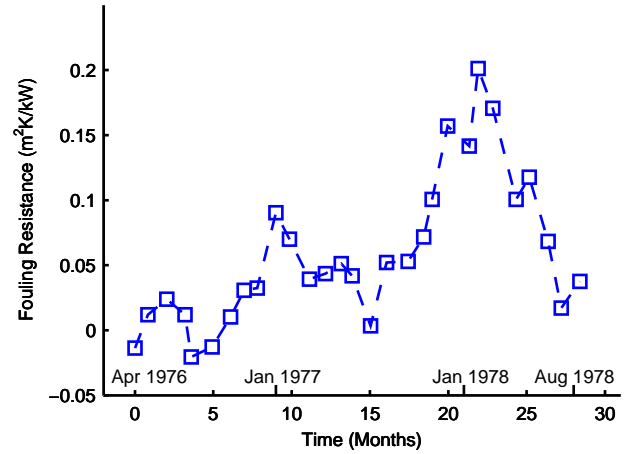


**FIGURE 13.** FOULING RESISTANCE OF GALLATIN STATION UNIT 1 CONDENSER [18]. The data shows that the condenser began operation in April 1975 after being cleaned to restore its condition, and taken off-line two years later in August 1978. Significant fluctuation in the fouling resistance is present, and is believed to be the result of seasonal variation of river water temperature. Negative fouling resistances are observed. This could be the result of sensor noise, and that small amount of fouling actually improves tube smoothness and its heat transfer rate [17].

criteria results in the following observations:

1. High prediction update frequency ($F_U$) and the number of data points per update ($N_f$) should be used to ensure accurate predictions can be made quickly, but increasing the update and sampling frequencies too high diminishes the the improvement.
2. Noise removal in the fouling resistance monitoring process is critical.
3. The model probability based on information criterion gives a reliable indication of the optimal model in the pool of hypothetical models.
4. The prognosis criterion $R_{PC}$ will have high fluctuation even when the model probability criterion has selected the best model. This fluctuation is an indication of the accuracy of prediction.

### Prognosis Using Power Plant Condenser Data

Little data on fouling in desalination plants is publicly available in the literature. However, Tennessee Valley Authority collected significant amount of fouling data at their power-plant condensers from fresh water river in the 1970s [18]. Fig. 13 shows the data that were available in one of their published studies. We have drawn on this data to test the performance of the proposed prognosis procedure.

The pool of possible fouling models is assembled to contain the linear, falling-rate, and asymptotic models described in the introduction. The initial deposition time $t_d$ is ignored, and an extra free parameter is added at the end as a constant since the condenser fouling data does not start at zero. The model

uncertainty is assumed to be a normally distributed random variable. An extra hypothetical model $f_4$ is included which has the form of a linear function multiplied by a sinusoid of period 12 months. The reason for including a sinusoid is the apparent seasonal dependence observed in the condenser unit, evident by the distinguishable peaks and troughs in the fouling curve at February and August of each year [18], and the combination of a linear function multiplied by sinusoid plus constant uncertainty seem to match the data well compared to other combinations of sinusoidal models.

$$f_1 : R_f(t) = \mathcal{N}(a_1, b_1)(t) + c_1 \tag{22}$$

$$f_2 : R_f(t) = \mathcal{N}(a_2, b_2) \log(c_2 t + 1) + d_2 \tag{23}$$

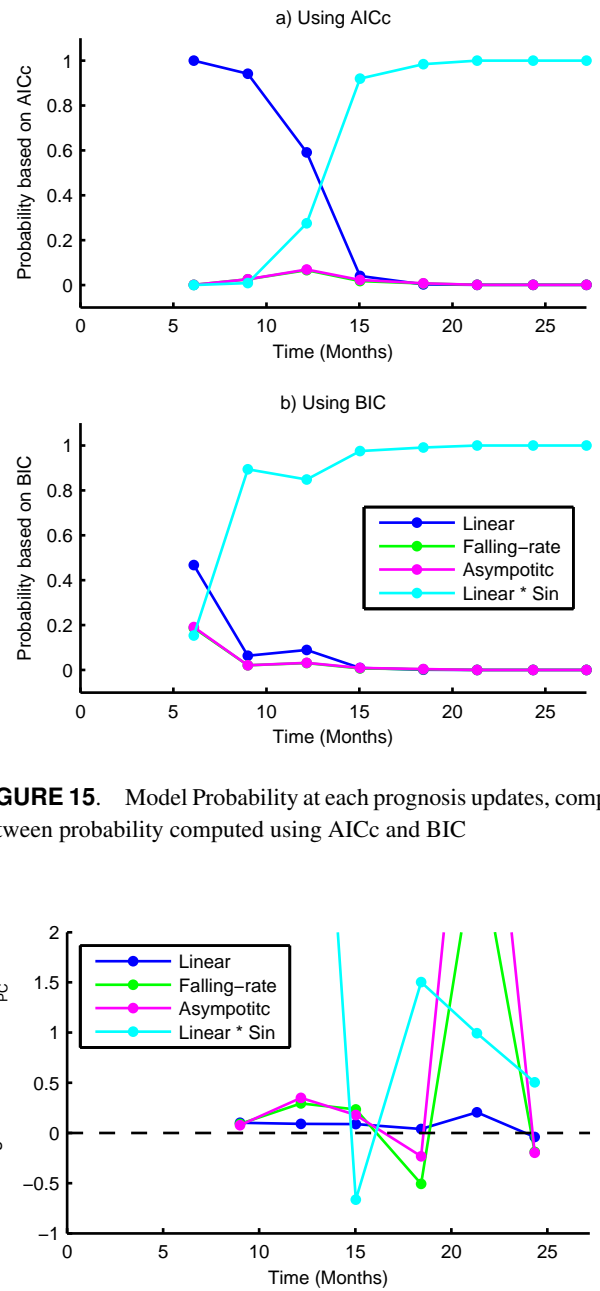$$f_3 : R_f(t) = \mathcal{N}(a_3, b_3)(1 - e^{-c_3 t}) + d_3 \tag{24}$$

$$f_4 : R_f(t) = \left[ a_4 + b_4 \sin\left(\frac{2\pi}{12} t + c_4\right) \right] t + \mathcal{N}(d_4, e_4) \tag{25}$$

In total, there are 29 fouling resistance data points sampled at a frequency of roughly once per month. A minimum of 6 initial sample points ($N_i = 6$) are needed to calculate meaningful AICc values using Eqn. 5. The number of samples per update $N_f$ is chosen to be 3, this will result in about 8 prognosis updates in the two year period. An $N_f$ value that is too high results in too
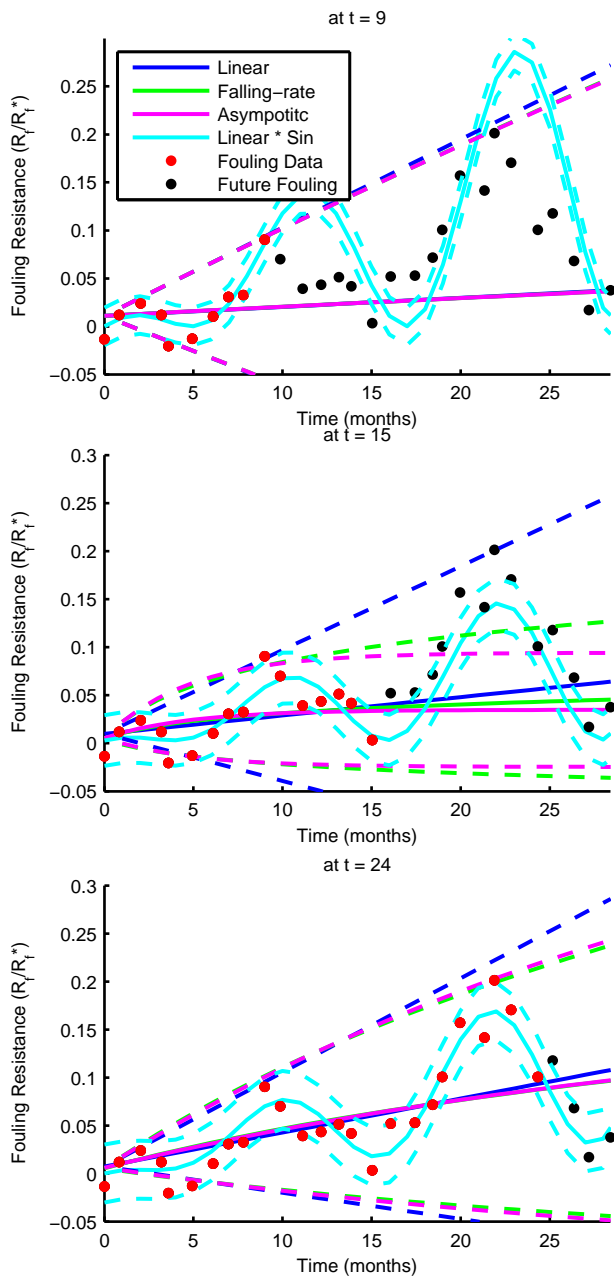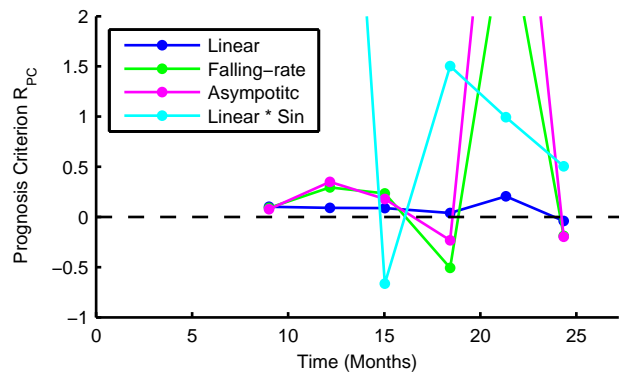
**FIGURE 14**. MAXIMUM LIKELIHOOD ESTIMATION OF CONDENSER FOULING MODELS AT THREE DIFFERENT TIMES. Dashed lines show the 5-95 percentile uncertainty region.



**FIGURE 15**. Model Probability at each prognosis updates, comparing between probability computed using AICc and BIC



**FIGURE 16**. Prognosis criterion at each prognosis updates

few prognosis updates, while $N_f$ too low can result in fluctuating prognoses. Fig. 14 shows the model estimation at different times. At the beginning with a small sample, the linear×sine model seem to over fit the data. The other three models all have

time-dependent uncertainty and thus predicted with a very wide uncertainty region. The model plots also suggest that falling-rate and asymptotic models are not good representations of the data because they are nearly identical and very similar to the linear model in shape.

Figure 15 shows the model probabilities calculated from the information criteria at each prognosis update. The probabilities

computed from AICc and BIC generally agree but have some discrepancies initially with time less than 10 months. When the sample size is small, AICc has a higher penalty for free parameters compared to BIC, and thus tends to pick the linear model that has fewer free parameters. The disagreement between AICc and BIC is a good indication that the confidence of prognosis is low for this set of data. The probabilities of the asymptotic model and the falling-rate model are very low for all times, suggesting they are not good representations of the data.

The prognosis criterion $R_{PC}$ at each update are shown in Fig. 16. Of the four models, only the linear model ($f_1$) showed a steady decline in its prognosis criterion, while the linear×sine model has a fluctuating $R_{PC}$ despite the high model probability. This situation is very similar to the scenario of contradicting criteria, and thus suggesting that making a prediction using the linear×sine model under this circumstances may be unreliable. More data points would be necessary to result in a reliable prediction of future degradation.

## CONCLUSIONS AND FUTURE WORK

In this work we proposed and studied a prognosis scheme for predicting future degradation in an engineering system by continuously monitoring of current degradation. We introduced the notion of a pool of hypothetical degradation models, a model selection criterion based on Akaike's and Bayesian Information Criteria, and a measure of the prognosis accuracy by computing the prognosis criterion. The performances of the method was analyzed with different operating parameters for a heat exchanger, and under non-ideal conditions. The process is also tested using condenser fouling data obtained from a real power plant. The results show that degradation prediction can be improved over continuous monitoring, and that increasing update frequency and samples per update will improve prediction confidence.

This study is the first step to the development of a monitoring and prognostic paradigm. Future degradation predicted using this scheme can be incorporated into a performance objective function, along with the model probabilities and prognosis criterion, to be optimized by strategic scheduling of maintenance. Extensions to this work would first focus on obtaining a performance objective function based on deterministic degradation only, and later optimize the objective function to include the accuracy criteria.

## ACKNOWLEDGMENT

## REFERENCES

[1] Boyce, M. P., 2002. *Handbook for Cogeneration and Combined Cycle Power Plants*. ASME Press.

[2] Dekker, R., 1996. "Applications of maintenance optimization models: A review and analysis". *Reliability Engineering & System Safety,* **51**(3), pp. 229–240.

[3] Schwabacher, M. A., 2005. "A survey of data-driver prognostics". In Infotech@Aerospace.

[4] Farrar, C. R., and Lieven, N. A. J., 2007. "Damage prognosis: the future of structural health monitoring". *Phil. Trans. of the Roya Society A-Mathematical Pysical and Engineering Sciences,* **365**(1851), pp. 623–632.

[5] Saha, B., and Goebel, K., 2009. "Modeling li-ion battery capacity depletion in a particle filtering framework". In Annual Conference of the Prognostics and Health Management Society.

[6] Kothamasu, R., Huang, S., and VerDuin, W., 2006. "System health monitoring and prognostics — a review of current paradigms and practices". *The International J. of Adv. Manufacturing Technology,* **28**, pp. 1012–1024.

[7] Chiang, L., Russel, E., and Braatz, R., 2001. *Fault detection and diagnosis in industrial systems*. London: Springer-Verlag.

[8] Wang, P., and Coit, D. W., 2006. "Reliability and degradation modeling with random or uncertain failure threshold". In 53rd Annual Reliability and Maintainability Symposium, IEEE, pp. 392–397.

[9] Lu, C. J., and Meeker, W. Q., 1993. "Using degradation measures to estimate a time-to-failure distribution". *Technometrics,* **35**(2), pp. pp. 161–174.

[10] Zuo, M., Jiang, R., and Yam, R., 1999. "Approaches for reliability modeling of continuous-state devices". *IEEE Transactions on Reliability,* **48**(1), MAR, pp. 9–18.

[11] Zhou, R. R., Serban, N., and Gebraeel, N., 2011. "Degradation Modeling Applied to Residual Lifetime Prediction using Functional Data Analysis". *Annals of Applied Statistics,* **5**(2B), JUN, pp. 1586–1610.

[12] Zubair, S., Sheikh, A., Budair, M., and Badar, M., 1997. "A maintenance strategy for heat transfer equipment subject to fouling: A probabilistic approach". *Journal of Heat Transfer-Transactions of the ASME,* **119**(3), pp. 575–580.

[13] Sheikh, A. K., Zubair, S. M., Younas, M., and Budair, M. O., 2001. "Statistical aspects of fouling processes". *Proc. Institution of Mechanical Engineers, Part E: Journal of Process Mechanical Engineering,* **215**(4), pp. 331–354.

[14] Prasad, V., Osborn, M. D., Au, S. S., Reddy, K. R. C., Shah, S. S., Vora, N. P., and Gryscavage, A., 2005. "Predic-

tive heat exchanger efficiency monitoring". In Proc. ASME Summer Heat Transfer Conference, ASME, pp. 281–290.

[15] Müller-Steinhagen, H., 2011. "Heat transfer fouling: 50 years after the kern and seaton model". *Heat Transfer Engineering,* *32*(1), pp. 1–13.

[16] Putman, R., and Walker, R., 2000. "Proper maintenance practices involving condenser cleaning and in-leakage inspection". In International Conference on Power State Maintenance, pp. 161–170.

[17] Epstein, N., 1983. "Thinking about heat transfer fouling: A 5 5 matrix". *Heat Transfer Engineering,* *4*(1), pp. 43–56.

[18] Rabas, T. J., Panchal, C. B., Sasscer, D. S., and Schaefer, R., 1993. "Comparison of river-water fouling rates for spirally indented and plain tubes". *Heat Transfer Engineering,* *14*(4), pp. 58–73.

[19] Taborek, J., Aoki, T., Ritter, R., Palen, J., and Knudsen, J., 1972. "Heat-transfer 2. predictive methods for fouling behavior". *Chemical engineering progress,* *68*(7), pp. 69–78.

[20] Kakac, S., 1991. *Boilers, Evaporators, and Condensers*. John Wiley & Sons, Inc.